
CDS - CAUSAL INFERENCE WITH DEEP SURVIVAL MODEL AND TIME-VARYING COVARIATES

A PREPRINT

Jie Zhu*

Centre for Big Data Research in Health (CBDRH)
UNSW, Sydney
NSW, 2052, Australia
elliott.zhu@unsw.edu.au

Blanca Gallego

Centre for Big Data Research in Health (CBDRH)
UNSW, Sydney
NSW, 2052, Australia
b.gallego@unsw.edu.au

October 11, 2021

*Corresponding Author

ABSTRACT

Objective Causal inference in longitudinal observational health data often requires the accurate estimation of treatment effects on time-to-event outcomes in the presence of time-varying covariates. To tackle this sequential treatment effect estimation problem, we have developed a causal dynamic survival (CDS) model.

Materials and Methods CDS estimates potential hazard functions under time-varying binary treatments using an ensemble of recurrent deep subnetworks. Following the potential outcomes framework, treatment effects are estimated as the difference in survival probabilities between the given treatment and control regimes. The ensemble training is used to capture the uncertainty of network estimation from varying random seeds, and a dedicated propensity score layer is used to adjust the selection bias presented in the data.

Results Using simulated survival datasets, the CDS model showed good causal effect estimation performance across scenarios of varying sample dimensions, event rate, confounding, and overlapping. However, increasing the sample size was not effective in reducing the bias from a high level of confounding. In two large clinical cohort studies, our model identified the expected conditional average treatment effects and detected individual treatment effect heterogeneity over time.

Discussion The use of a propensity score layer and potential outcome subnetworks helps correcting for selection bias. However, the proposed model is limited in its ability to correct the bias from unmeasured confounding, and more extensive testing of CDS under extreme scenarios such as low overlapping and the presence of unmeasured confounders is desired and left for future work.

Conclusion CDS fills the gap in causal inference using deep learning techniques in survival analysis. It considers time-varying confounders and treatment options. Its treatment effect estimation can be easily compared with the conventional literature, which uses relative measures of treatment effect. We expect CDS will be particularly useful for identifying and quantifying treatment effect heterogeneity over time under the ever complex observational health care environment.

Keywords Survival Analysis · Causal Inference · Machine Learning · Neural Subnetworks

1 Background and Significance

While randomized experiments are the gold standard in the comparison of interventions, it has become clear that observational studies using Big Data have an important role to play in comparative effectiveness research [1]. As a result, the last few years have seen a surge of studies proposing and comparing methods that can estimate the effect of interventions from routinely collected data. In particular, new methods have emerged that can investigate the heterogeneity of the treatment effect. In the health domain, these methods use Medical Claims [2] and Electronic Health Record (EHR) data and have been driven by the move towards personalized care [3].

In spite of significant progress, there remain challenges that must be addressed. In particular, no off-the-shelf treatment effect algorithm exists that takes full consideration of the temporal nature of medical data including: patient history, time-varying confounders, time-varying treatment and time-to-event outcomes. Accounting for the temporal nature of medical information is important when informing clinical guidelines or designing clinical decision support systems, since they underpin clinicians’ response to disease progression and patient deterioration.

As a motivating example, early detection and treatment of sepsis are critical for improving sepsis outcomes, where each hour of delayed treatment has been associated with roughly a 4-8% increase in mortality [4]. To help address this problem, clinicians have proposed new definitions for sepsis [5], but the fundamental need to detect and treat sepsis early still remains. In this context, time-dependent confounders such as the count of white blood cells, partial pressure of oxygen (PaO_2) and fraction of inspired oxygen (FiO_2) will be affected by the previous administration of antibiotics or use of mechanical ventilation (MV). Similarly, the treatment effects in chronically ill patients (such as Atrial Fibrillation or Diabetes) changes with shifts in the patient’s risk profile and accumulates over time. The challenge of capturing the history of time-varying biomarkers and other risk factors pervades the prediction of time-to-event outcomes and the associated treatment effects in the clinical decision process.

Our aim, therefore, is to use longitudinal health record data to predict the risk of a target outcome in terms of survival probability and to estimate the corresponding survival treatment effect for individuals or patient groups. The standard approach hinges on outcome models that learn from a snapshot of baseline covariates and a static binary treatment assignment. When required, the temporality starting from the initiation of the follow-up is incorporated ‘manually’, for example, by defining maximum, cumulative or average values over time.

Several recent papers have described extensions of static survival outcome models [6, 7] to predict longitudinal time-to-event outcomes, including methods such as Longitudinal Targeted Maximum Likelihood Estimation (LTMLE) [8] and Dynamic DeepHit [9]. However, LTMLE fails to incorporate the dimensionality and complexity of EHR data, while Dynamic DeepHit does not capture the causal effect on the longitudinal survival outcomes.

Conventionally, hazard ratio (HR) is used as the effect measure in causal inference on time-to-event outcomes. Despite the potential violation of the constant HR assumption in the Cox model, it is hard to interpret HR due to selection bias as the susceptible individuals used to calculate HR are depleted under different rates between the treatment and control groups. As an alternative, in this study we estimate the absolute treatment effect in terms of the difference in the potential survival curves under treatment or control conditions at the individual level [10].

To estimate the absolute treatment effect, the potential survival probabilities in the control and treatment groups are modeled using a novel deep learning estimation of the time-to-event (survival) outcomes. The potential difference in individual survival curves under treatment and control conditions is estimated given the observed history and treatment assignment. We call this model Causal Dynamic Survival Model (CDS).

The key characteristics of the proposed algorithm are: 1) it learns the treatment assignment and outcome generating process from the pattern of observed and missing covariates in longitudinal data; 2) it captures treatment specific risks by employing potential outcome subnetworks for treatment and control conditions; and 3) it quantifies the uncertainty of the model estimations with an ensemble of neural networks with varied random seeds.

The outline of this paper is as follows. Section 2 describes the methodology to estimate the longitudinal survival outcomes and treatment effect. In Section 3, we introduce a set of simulation studies, case studies, and model evaluation techniques. Section 4 provides the results. We end with a discussion.

2 Materials and Methods

2.1 Related works

We focus on methods for estimating survival outcomes and treatment effects over time with time-varying covariates.

The standard method to estimate the treatment effect with time-varying covariates, such as landmark analysis [11], uses the Cox model [12]. In this landmark analysis, the instantaneous probability of experiencing an event at time t given covariates $X(t)$ is defined as a hazard function: $h(t|X(t)) = h_0 \exp(\beta' X(t))$, where β is a vector of constants, and h_0 is the baseline risk of having an event at time 0. When censoring is not considered, a Cox model compares the risk of an event between treatment and control conditions at each time t regardless of previous history of $X(t)$ or history of treatment conditions. The piece-wise constant Cox model [13] extends the constant β to $\beta(t)$ thus allowing for time-varying effect. However, neither model takes into account the longitudinal history of covariates and both treat missing covariates either by imputing their value or removing the incomplete observations.

To address these limitations, models were proposed to jointly describe both longitudinal and survival processes [14, 15]. In particular, these joint models generally comprise two submodels: one for repeated measurements of time-varying covariates and the other for time-to-event data such as a Cox model. The models are linked by a function of shared random effects. To find a full representation of the joint distribution of the two processes, the model needs to be correctly specified for both processes. Thus, model misspecification and computation efforts significantly limit the estimation accuracy of this approach when applied to high-dimensional EHR data.

Recently, data-driven models such as recurrent neural networks [16, 9] have been proposed to learn efficiently from EHR data with complex longitudinal dependencies. For example, Dynamic DeepHit [9] is a longitudinal outcome model which learns the joint distribution of survival times and competing events from a sequence of longitudinal measurements with a recurrent neural network structure. As a single outcome prediction model, DeepHit does not provide an explanatory mechanism for causal inference.

On the other hand, the Counterfactual Recurrent Network (CRN) [16] estimates the average longitudinal treatment effect on continuous outcomes by correcting for time-varying confounding using domain adversarial training (DAT). However, the efficacy of DAT depends on the feature alignment in the source (control) and target (intervention) domains [17], that is, whether the covariates observed under treatment and control conditions have similar distributions. As shown in the original work, the DAT is sensitive to the overlapping among covariates and drops in estimation performance with the level of overlapping like other existing causal inference algorithms such as the TMLE [7] and Causal Forest [18].

There is a lack of studies dedicated to estimating survival causal effects from longitudinal EHR data. We fill in this gap by extending our previous work on modeling the treatment effect on time-to-event outcomes from static covariates [19] to time-varying (longitudinal) covariates. We choose an ensemble of recurrent neural networks as the outcome model. Neural networks learn more efficiently from the trajectories of covariates than semi-parametric or parametric methods such as Super-learner and Cox models, while the ensemble captures the uncertainty of network estimation. Both the baseline survival probability and its interaction with treatment can vary with time free from the proportional hazard assumption.

In lieu of a single outcome model (like DeepHit) for estimating the joint distribution of the observed failure/censor times, CDS (see Figure 1) first captures the information from treated and control observations separately, and then encodes it into a shared subnetwork. The encoded information is fed into counterfactual subnetworks to predict the expected survival outcomes given either treatment or control conditions. The dedicated subnetworks explicitly model the risks originated from patient baseline covariates and their interaction between treatment conditions.

Lastly, we adjust for bias in the counterfactual outcomes arising from nonrandom treatment allocation in observational studies. The difference between the counterfactual survival probabilities will give us calibrated treatment effect estimates. In the rest of this section, we formally define the research problem and explain the construction of CDS.

2.2 Building the model

This section describes the CDS model introduced in Figure 1. To formalize the framework for causal inference on longitudinal survival outcomes, we follow the notations in previous studies [20, 19]. Suppose we observe a sample \mathcal{O} of n independent observations generated from an unknown distribution \mathcal{P}_0 :

$$\mathcal{O} := (X_i(t), Y_i(t), A_i(t), \tau_i = \min(\tau_{s,i}, \tau_{c,i})), i = 1, 2, \dots, n$$

where $X_i(t) = (X_{i,1}(t), X_{i,2}(t), \dots, X_{i,d}(t))$, $d = 1, 2, \dots, D$ are confounders at time t ; $t = 1, 2, \dots, t', \dots, \Theta$, where t' denotes the start of follow-up and Θ is the study's maximum follow-up time; and $A_i(t)$ is the treatment condition at time t , which can take the value of 0 or 1 for control and treatment conditions respectively. Both $X_i(t)$ and $A_i(t)$ are captured from $t' - u$ to $t' - 1$ (inclusive), that is, u is the length of the patient's history window. Lastly, $Y_i(t)$ denotes the outcome at time t , $Y_i = 1$ if i experienced an event and $Y_i = 0$ otherwise. The end of follow-up for a given patient, τ_i , $\tau_i \geq t'$, is determined by the event or censor time, $\tau_{s,i}$ or $\tau_{c,i}$, whichever happened first. For simplicity, we drop the subscript i in the sequel.

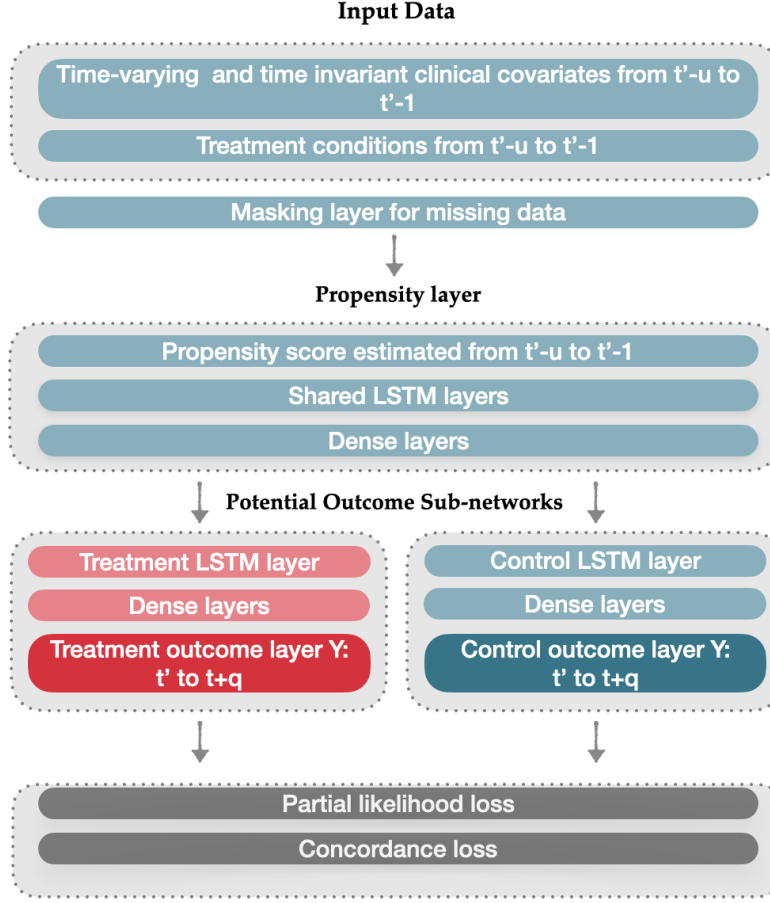


Figure 1: Illustration of the causal dynamic survival model (CDS) Abbreviations: t' , the commencement of the estimation period; $t' + q$, the lead time (where q is the length of estimation window); $t' - u$, the history (where u is the length of the history window)

In Figure 3, the input data of Figure 1 is organised into a matrix of observed confounders from $t' - u$ to $t' - 1$. This longitudinal matrix is first used to estimate the propensity of receiving the treatment via a densely connected neural network with Long Short-Term Memory [21] (LSTM) units. The output of this network is the conditional propensity of receiving the treatment $A = a$ at time t :

$$p(a(t)|x(t)) := \Pr(A(t) = a(t)|X(t) = x(t)),$$

where $a \in \{0, 1\}$ and $t \in \{t' - u, t' - u + 1, \dots, t' - 1\}$.

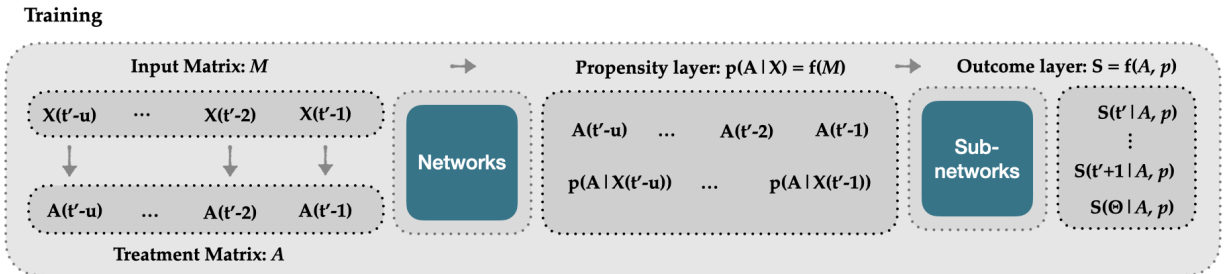


Figure 2: Training pipeline of the causal dynamic survival model (CDS).

Next, the estimated propensity scores and the observed treatment conditions are used as the input of the potential outcome subnetworks to estimate the survival curves². In order to compute the survival probabilities from t' to Θ , we first define the conditional hazard rate $h(\tau), \tau \geq t'$, the probability of experiencing an event in interval $(\tau - 1, \tau]$, as:

$$h(\tau, a(u)) := \Pr(Y(\tau) = 1 \mid \bar{A}(u) = a(u), p(a(u) \mid \bar{X}(u))),$$

where $\bar{A}(u)$ and $\bar{X}(u)$ are the matrices of observed treatments and estimated conditional propensity scores during the history window from $t' - u$ to $t' - 1$. Thus, the probability that an uncensored individual will experience the event in period τ conditioned on treatment history $a(u)$ can be written as a product of terms, one per period, describing the probability that the event did not occur since time τ to $\tau - 1$ but occur in period $(\tau - 1, \tau]$:

$$\begin{aligned} \Pr(\tau_s = \tau \mid a(u)) &= h(\tau, a(u))(1 - h(\tau - 1, a(u)))(1 - h(\tau - 2, a(u))) \cdots (1 - h(t', a(u))) \\ &= h(\tau, a(u)) \prod_{j=t'}^{\tau-1} (1 - h(j, a(u))). \end{aligned}$$

Similarly, the probability that a censored individual will experience an event after time τ can be written as a product of terms describing the conditional probability that the event did not occur in any observation:

$$\begin{aligned} S(t = \tau, a(u)) &= \Pr(\tau_s > \tau \mid a(u)) \\ &= (1 - h(\tau, a(u)))(1 - h(\tau - 1, a(u)))(1 - h(\tau - 2, a(u))) \cdots (1 - h(t', a(u))) \\ &= \prod_{j=t'}^{\tau} (1 - h(j, a(u))). \end{aligned} \tag{1}$$

which is also the survival function.

The CDS model estimates Equation 1 with a dedicated neural network which regresses the trajectory of historical treatments $\bar{A}(u)$ and the estimated propensity scores $p(\bar{A}(u) \mid \bar{X}(u))$ on the outcome label Y^M , defined as a matrix over $\tau \in \{t', t' + 1, \dots, \Theta\}$:

$$Y^M = \begin{bmatrix} E \\ C \end{bmatrix},$$

where

$$\begin{aligned} E &= [e_i(t'), e_i(t' + 1), \dots, e_i(\tau), \dots, e_i(\Theta)] \\ e(\cdot) &= 1 \text{ for } t' < \tau \text{ if a patient is censored or having an event at } \tau \\ e(\cdot) &= 0 \text{ for } t' \geq \tau; \\ C &= [c(t'), c(t' + 1), \dots, c(\tau), \dots, c(\Theta)] \\ c(\cdot) &= 0 \text{ if a patient is censored at } \tau; \\ c(\cdot) &= 0 \text{ and } c(\tau) = 1 \text{ if a patient is having an event at } \tau. \end{aligned} \tag{2}$$

This gives us a Θ -dimensional vector \hat{H}_Θ with each element representing the estimated conditional probability of surviving a time interval: $1 - \hat{h}(t, a(u))$. Then the estimated survival probability will be given by $\hat{S}(t, a(u))$. In the next section, we describe how to use the potential survival probabilities estimated by CDS to compute the debiased estimation of the conditional average treatment effect (CATE) curve.

2.3 Definition of survival treatment effect with longitudinal data

To estimate the treatment effect curve, we follow Rosenbaum and Rubin's potential outcomes framework [22], and assume 1) the censoring is non-informative conditioned on the treatment (coarsening at random), 2) there is no

²Please see Appendix B for the descriptions of the layers contained in the network.

unmeasured confounders, and 3) the history of treatment assignment $\bar{A}(u)$ is independent of the survival curve given the history of confounders $\bar{X}(u)$:

$$\mathbb{E}[S(t, a(u)) | A = a(u), p(A = a(u) | X(u))] = \mathbb{E}[S(t, a(u)) | p(A = a(u) | X(u))],$$

for $t \in \{t', t' + 1, \dots, \Theta\}$. Under these assumptions, the conditional average treatment effect (CATE) is defined as:

$$\Psi(t, \bar{x}(u)) = \mathbb{E}_{\bar{X}(u)=\bar{x}(u)} [\mathbb{E}[S(t, 1) | \bar{A}(u) = 1, \bar{X}(u) = \bar{x}(u)] - \mathbb{E}[S(t, 0) | \bar{A}(u) = 0, \bar{X}(u) = \bar{x}(u)]]$$

where $\bar{A}(u) = 1$ means the patient would be under the treatment from $t' - u$ to $t' - 1$ and $\bar{A}(u) = 0$ means the patient would be under control during the same historical period. Similarly, we define the individual treatment effect (ITE) as:

$$\psi(t, \bar{x}(u)) = \mathbb{E}[S(t, 1) | \bar{A}(u) = 1, \bar{X}(u) = \bar{x}(u)] - \mathbb{E}[S(t, 0) | \bar{A}(u) = 0, \bar{X}(u) = \bar{x}(u)] \quad (3)$$

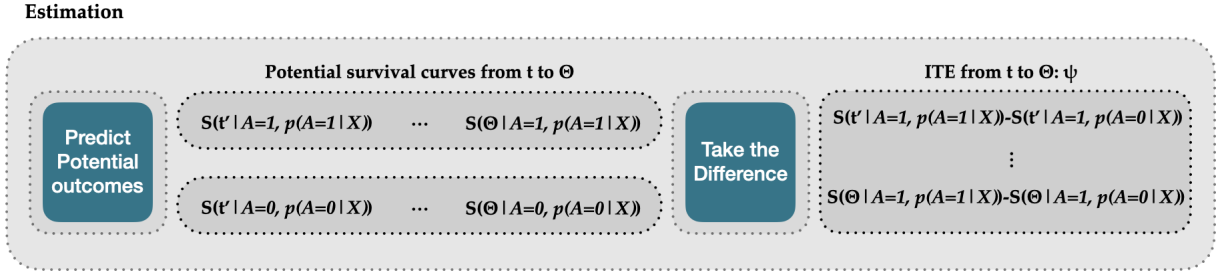


Figure 3: Estimation pipeline of the causal dynamic survival model (CDS).

As illustrated in Figure 3, the trained CDS model is used to estimate the potential outcomes, $\hat{S}(t, 1)$ (intervention) and $\hat{S}(t, 0)$ (control/comparator), conditioned on treatment and confounders during the history window, and then computes the quantity given in Equation (3).

To compare the absolute measure of treatment effect with the conventionally reported hazard ratio, we define an empirical hazard ratio as:

$$\text{HR}^*(t, \bar{x}(u)) = \frac{1}{n} \sum_i \frac{\hat{h}_i(t | \bar{A}(u) = 0, \bar{X} = \bar{x}(u))}{\hat{h}_i(t | \bar{A}(u) = 1, \bar{X} = \bar{x}(u))} \quad (4)$$

where n is the number of observations in a sample.

2.3.1 The loss function

To train our neural network, we vectorized each individual event/censoring time to construct the target outcome in Equation (2) and apply a loss function with two components (the condition indicators $\bar{A}(u)$ and $\bar{X}(u)$ are dropped in the sequel):

1) the partial log likelihood loss of the joint distribution of the first failure time and the corresponding event or censoring over time:

$$\mathcal{L}_1 = \sum_i \left[\ln(C_i \hat{H}_{i,\Theta}) + \ln(E_i \hat{H}_{i,\Theta}) \right]$$

which is a vector representation of the ordinary partial log-likelihood loss:

$$\mathcal{L}_{\text{uncensored}} = \sum_i c_i \left[\ln(h_i(t)) + \sum_{j=0}^{t_i-1} \ln(1 - h_i(j)) \right]$$

$$\mathcal{L}_{\text{censored}} = \sum_i (1 - c_i) \left[\sum_{j=0}^{t_i-1} [1 - h_i(j)] \right], \text{ where } c_i = 1 \text{ if } i \text{ is event happened, and } c_i = 0 \text{ otherwise;}$$

Then \mathcal{L}_1 can be written as:

$$\begin{aligned} \mathcal{L}_1 &= \mathcal{L}_{\text{uncensored}} + \mathcal{L}_{\text{censored}} \\ &= \sum_i \left[c_i \ln(h_i(t_i)) + c_i \sum_{j=0}^{t_i-1} \ln(1 - h_i(j)) + (1 - c_i) \sum_{j=0}^{t_i-1} \ln(1 - h_i(j)) \right] \\ &= \sum_i \left[c_i \ln(h_i(t_i)) + \sum_{j=0}^{t_i-1} \ln(1 - h_i(j)) \right] \end{aligned}$$

2) the rank loss function to capture the concept of concordance in survival analysis [23]: a subject who experienced an event at time t should have a higher probability of failure than a subject who doesn't or who is censored. We count the number of acceptable pairs of estimated hazard rate $\{\hat{h}_i(t), \hat{h}_j(t)\}$ in the loss function:

$$\mathcal{L}_2 = \sum_t \sum_{i \neq j} I_{ij}$$

where I_{ij} is an indicator function:

$$I_{ij} = 1, \text{ if } Y_i(t) = 1, Y_j(t) = 0 \text{ and } \hat{h}_i(t) > \hat{h}_j(t),$$

$I_{ij} = 0$, otherwise.

The final loss function is defined as:

$$\mathcal{L} = \alpha \mathcal{L}_1 + \beta \mathcal{L}_2,$$

where random search is used to locate the best hyper-parameters α and β . To capture the uncertainty of the neural network, we iterate the model training with different random seeds for 20 iterations and average the results from each training.

2.4 Simulation design

To explore the finite-sample performance of CDS, we ran several experiments with biologically plausible longitudinal data following a previous study [24]. In particular, we use:

- D continuous confounders $X(t)_1, X(t)_2, \dots, X(t)_D \sim N(\sqrt{t}, V)$ from $t = t' - u$ to $t = t' - 1$, where V is variance of the normal distribution and D is the feature dimension;
- Binary exposure: $A(t) \sim \text{Binom}(\eta \cdot I(\sum_{d=1}^3 X(t)_D > \frac{1}{3} \sum_{i=1}^3 X(t)_i) + 0.5 \cdot (1 - \eta))$, where I is an indicator function and η controls the level of overlapping. When $\eta = 0$, the probability of receiving the treatment is 50% regardless of $X(t)$; when $\eta = 1$, the allocation follows the indicator function so that the outcome will be confounded by the first 3 confounders of $X(t)$; and when $\eta = 0.5$, the chance of receiving the treatment is partially dependent on the indicator function which is $(0.5 \cdot I + 0.25)100\%$.
- Hazard rate: $h(t) = \frac{\log(t)}{\lambda} (0.1A(t) + \beta \sum_{i=1}^D X(t)_i)$ where $\beta = 1$;
- The survival probability $S(t) = \exp(-h(t))$;
- The censoring probability $SC(t) = \exp(-\frac{\log(t)}{\lambda})$, where $\lambda = 30$;
- An event indicator generated using *root-finding* [24] at each time t : $E(t) = I(S(t) < U \sim \text{Uniform}(0, 1))$, with the event time defined by τ_s if $E_i(\tau_s) = 1$, otherwise $\tau_s = \Theta + 1$;

- A censoring indicator generated using the *root-finding* technique: $C(t) = I(SC(t) < U \sim \text{Uniform}(0, 1))$, with the censoring time defined by τ_c if $C(\tau_c) = 1$, otherwise $\tau_c = \Theta$, and;
- The survival outcome given by the indicator function: $Y = I(\tau_s \leq \tau_c)$.

A series of experiments were conducted by changing the following parameters: $V \in \{0.5, 1.0, 1.5, 2.0\}$, $D \in \{6, 10, 20, 40\}$, $\eta \in \{0.7, 0.8, 0.9, 1.0\}$, $N \in \{1500, 3000, 10000\}$. We define our default data generation model with $V = 0.5$, $D = 6$, $\eta = 0.9$, and $N = 1500$. In this study, we set the length of the estimation window from t' to Θ at 10 time steps and the length of history window at five time steps ($u = 5$). For each scenario, we generate 50 sets of training and testing samples using the same parameters but different random seeds. All evaluations are averaged over the testing results from these 50 samples.

2.5 Case studies

We built and then applied our model to two clinical causal inference questions:

1. Effect of mechanical ventilation (MV) on in-hospital mortality for sepsis patients in the ICU. The data source for this case study is MIMIC-III, an open-access, anonymised database of 61,532 admissions from 2001–2012 in six ICUs at a Boston teaching hospital [25]. A sepsis event is defined as a suspected infection (prescription of antibiotics and sampling of bodily fluids for microbiological culture) combined with evidence of organ dysfunction, defined by a two-points deterioration of the SOFA score [26]. We follow previous papers [27, 28] for data extraction and processing. We define the treatment as the use of mechanical ventilation(MV), where previous literature has found a positive impact on patients' in-hospital mortality.
2. Comparative effectiveness of Vitamin K Antagonists (VKAs) and Non-Vitamin K antagonist oral anticoagulants (NOAC) in preventing three combined outcomes (ischemic event, major bleeding and death) for patients with non-valvular atrial fibrillation (AF). The data source for this case study is Clinical Practice Research Datalink (CPRD) [29] dataset. A detailed description of this cohort can be found in our working paper [30].

A summary of the clinical cohorts is presented in Table 1. We only consider the first 20 time stamps for each patient in each dataset (i.e., the first 20 2-hour intervals for MIMIC-III and the first 20 three-month intervals for the AF dataset.). We train the model using the 10-fold cross validation with 70% of the original data injected in each training epoch. We predict the average treatment effect estimation at each time step using the whole sample.

Table 1: Summary of case study databases

	MIMIC-III	AF
Unique patient ids	20,938	20,270
Number of event patients	2,880	3,215
Rows for the first 20 time stamp	278,504	150,193
Static features	5	49
Dynamic features	39	4

2.6 Model evaluation

The explanatory performance of CDS is assessed with simulation studies using the three metrics described below:

Root-mean-square error (RMSE): Refers to the expected mean squared error of the estimated individual treatment effect:

$$\text{RMSE}(t) = \frac{1}{n_k} \sum_{i_k} (\hat{\psi}_{i_k}(t) - \psi_{i_k}(t))^2$$

where n_k is the number of individuals in subgroup k and i_k is the individual indicator in each group. When estimating the ATE, we will have $n_k = N$, the sample size.

Absolute percentage bias (Bias): Defined as the absolute percentage bias in the estimated conditional average/individual treatment effect:

$$\text{Bias}(t) = \frac{1}{n_k} \sum_{i_k} \left| \frac{\hat{\psi}_{i_k}(t) - \psi_{i_k}(t)}{\psi_{i_k}(t)} \right|$$

Coverage ratio: Refer to the percentage of times that the true treatment effect lies within the 95% confidence intervals of the posterior distribution of the estimated individual treatment effect.

$$\text{Coverage}(t) = \frac{1}{n_k} \sum_{i_k} I(|\hat{\psi}_{i_k}(t) - \psi_{i_k}(t)| < CI_{i_k}(t))$$

where I is an indicator function, $I = 1$ if $I(\cdot)$ is true and 0 otherwise. CI is the 95% confidence interval of the estimations.

Concordance and AUROC: We evaluate the models' discrimination performance of the estimated survival curves with Harrell's Concordance-index [23] and the area under the receiver operating characteristic curve (AUROC).

2.6.1 Benchmark Algorithms

The CDS model was benchmarked against two other machine learning algorithms:

1. Plain recurrent neural network with survival outcomes (SNN): this is achieved by removing the propensity score estimation layer in Figure 1.
2. Plain recurrent neural network with binary outcomes (Binary): direct prediction of the longitudinal outcome defined by the independent Binary labels in the first part of Equation (2) using mean squared error as the loss function.

For a fair comparison, we applied the inverse probability weighting (IPW) and the iterative targeted maximum likelihood estimation (TMLE) to the raw estimations from SNN and Binary to correct for selection bias when estimating the CATE (please refer to Appendix A for a detailed explanation). We developed CDS using Python 3.8.0 with Tensorflow 2.5.0[31] (code available at <https://github.com/EliotZhu/CDS>).

3 Results

3.1 Experiments

In Table 2, we compare CDS against the selected benchmark models using the test data generated under the default scenario. The Binary method achieves the highest AUROC, while CDS and SNN models have better performance in concordance due to the survival outcomes design. In terms of treatment effect estimation, CDS achieves nominal performance in both ITE and ATE estimations compared to both IPW and TMLE adjusted ATE estimations provided by the Binary and SNN models.

Table 2: Estimation performance by benchmark algorithms under the default scenario

Metrics	Algorithms		
	Binary	CDS	SNN
AUROC	0.96 (0.816,1.106)	0.82 (0.729,0.914)	0.85 (0.725,0.983)
Concordance	0.76 (0.730,0.799)	0.90 (0.852,0.947)	0.86 (0.798,0.913)
Bias (IPW)	0.65 (0.625,0.675)	-	0.15 (0.133,0.167)
Bias (TMLE)	0.63 (0.576,0.684)	-	0.14 (0.129,0.151)
Bias (ATE)	-	0.10 (0.061,0.136)	-
Bias (ITE)	0.75 (0.706,0.794)	0.10 (0.064,0.137)	0.43 (0.401,0.459)

All metrics are averaged across 50 independent simulations over 30 time points from the test dataset under the default scenario.

The improvement of CDS is most noticeable in the estimation of the ITEs, where the Bias is only 0.10 (0.064,0.137) across 50 samples compared to 0.43 (0.401,0.459) of the SNN model. However, the improvement of ATE estimation by CDS compared to TMLE or IPW adjusted SNN estimation is less significant, at around 5%. CDS gains from its design of the propensity score layer as well as the potential outcomes subnetworks. In Figure 4, we illustrate how CDS provides ITE estimations close to the true values, unlike the Binary and the SNN models. In particular, the Binary model only maximises its discrimination performance in terms of AUROC but provides no value to the treatment effect estimation.

The performance of CDS over time is examined across different scenarios in Table 3. The performance of CDS stands out when there is perfect overlapping ($\eta = 1$). In this case, the bias (as well as RMSE) of ATE and ITE estimations are

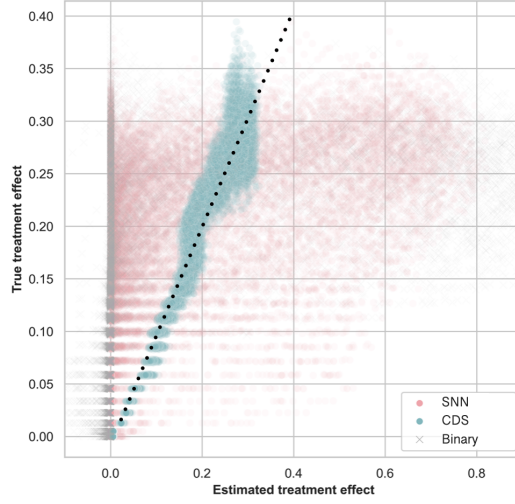


Figure 4: Diagnostic plots for the CDS model. True and estimated individual treatment effect (ITE) distributions by benchmark algorithms. The colored dots are the true and estimated ITE averaged over of a randomly chosen sample under the default scenario. The dashed diagonal line indicates the equation of the true and estimated values.

Table 3: Simulation study results.

	Bias (ATE)	Coverage	Bias (ITE)	RMSE
Overlap (η)				
0.7	0.11 (0.070,0.157)	0.70 (0.644,0.756)	0.12 (0.081,0.167)	1.04 (0.630,1.420)
0.8	0.11 (0.063,0.151)	0.72 (0.618,0.824)	0.11 (0.063,0.151)	1.08 (0.367,1.801)
0.9	0.10 (0.061,0.136)	0.90 (0.804,0.995)	0.10 (0.064,0.137)	1.04 (0.330,1.743)
1	0.06 (0.012,0.107)	0.98 (0.953,1.000)	0.06 (0.014,0.106)	0.56 (0.119,1.003)
Dimension (D)				
6	0.10 (0.061,0.136)	0.90 (0.804,0.995)	0.10 (0.064,0.137)	1.04 (0.330,1.743)
10	0.09 (0.050,0.135)	0.94 (0.863,1.000)	0.08 (0.042,0.125)	1.05 (0.547,1.553)
20	0.10 (0.044,0.161)	0.94 (0.906,0.967)	0.10 (0.044,0.161)	1.29 (0.518,2.061)
40	0.08 (0.022,0.130)	0.93 (0.885,0.971)	0.08 (0.023,0.130)	1.09 (0.627,1.552)
Variance (V)				
0.5	0.10 (0.061,0.136)	0.90 (0.804,0.995)	0.10 (0.064,0.137)	1.04 (0.330,1.743)
1.0	0.10 (0.062,0.143)	0.96 (0.924,1.004)	0.10 (0.066,0.143)	1.02 (0.661,1.379)
1.5	0.11 (0.063,0.166)	0.83 (0.746,0.924)	0.12 (0.066,0.166)	1.21 (0.513,1.914)
2.0	0.08 (0.020,0.135)	0.87 (0.794,0.949)	0.10 (0.038,0.155)	1.10 (0.490,1.715)
Time				
1	0.10 (0.101,0.101)	0.88 (0.875,0.875)	0.10 (0.101,0.101)	0.10 (0.101,0.101)
5	0.09 (0.053,0.137)	0.94 (0.891,0.993)	0.10 (0.054,0.138)	0.94 (0.130,1.744)
10	0.10 (0.059,0.139)	0.89 (0.802,0.983)	0.10 (0.061,0.139)	1.16 (0.397,1.922)

All metrics are averaged across 50 independent simulations over 30 time points from the test dataset under the default scenario. The shaded row indicates the default scenario.

about half as that in the decreased overlapping scenarios. Similarly, coverage is close to perfect when $\eta = 1$, at 0.98 (0.953,1.005). As the degree of overlapping drops, there is no significant difference in estimation accuracy in terms of the Bias, but the coverage rate declines dramatically from 0.90 (0.804,0.995) when $\eta = 0.9$ to 0.70 (0.644,0.756) when $\eta = 0.7$ due to decreased confidence in individual estimations. CDS is stable over scenarios with different sample dimensions from the default 6 confounders to the high-dimension 40-confounder scenario. However, the estimation accuracy declines with higher sample variance, when the sample variance is high ($V = 2.0$), the coverage declined by about 3% to 0.87 (0.794,0.949) compared to the default scenario. Lastly, we found the confidence interval widens over time, but there is no deterioration in the effect estimation accuracy.

In Appendix C, we repeated the above scenarios with two additional sample sizes $N = 3000$ and $N = 10000$. We found larger sample sizes improve the estimation accuracy for more complex data (i.e., higher level of dimension and sample variance). However, they can not help to improve the estimation for samples that lack overlapping. For

observational EHR data, using a sample with moderate to high levels of overlapping is necessary to achieve better estimation accuracy.

3.2 Treatment effect estimation with clinical data

We applied CDS to two clinical causal inference questions. Figure 5 shows the estimation of ATE in terms of the differences in survival probability using CDS and SNN with TMLE adjustment (labeled as SNN+TMLE). We compared this absolute measure with the inversed empirical hazard ratio (i.e., $1/HR^*$, this is to make the hazard ratio in the same direction as the absolute difference in survival curves) and found that both curves closely follow each other.

In the MIMIC-III study[25] in panel (a) of Figure 5 focuses on the effect of using mechanical ventilation (MV) on the mortality of patients detected with sepsis. The first 12 hours of data were used to estimate the treatment effect of MV on patient mortality for the subsequent 40 hours. We found the empirical hazard ratio ranges from 0.975 to 0.992, suggesting a minimal positive impact of using mechanical ventilation. The estimation indicates that the usage of MV has its positive impact increasing over time and by the end of the follow-up period, we saw the usage of MV is expected to reduce the probability of death by 2.24% (1.26%, 7.23%) for CDS or 3.04% (2.11%, 6.54%) for TMLE.

Panel (b) illustrates the atrial fibrillation study which uses the CPRD dataset to compare the VKAs versus NOAC in preventing three combined safety and efficacy outcomes in patients with non-valvular atrial fibrillation (AF). Using the data collected during the first year (12 months) of follow-up, we observed an empirical hazard ratio ranging from 0.917 to 1.032 over the 48-month estimation period. The estimated ATE suggests that using VKA can improve the long-term outcome of patients by reducing the probability of combined outcomes up to 2.11% (-2.085%, 6.319%) (for the detailed study on the comparative effectiveness of NOAC vs VKA in non-valvular atrial fibrillation patients, please refer to our working paper [30]).

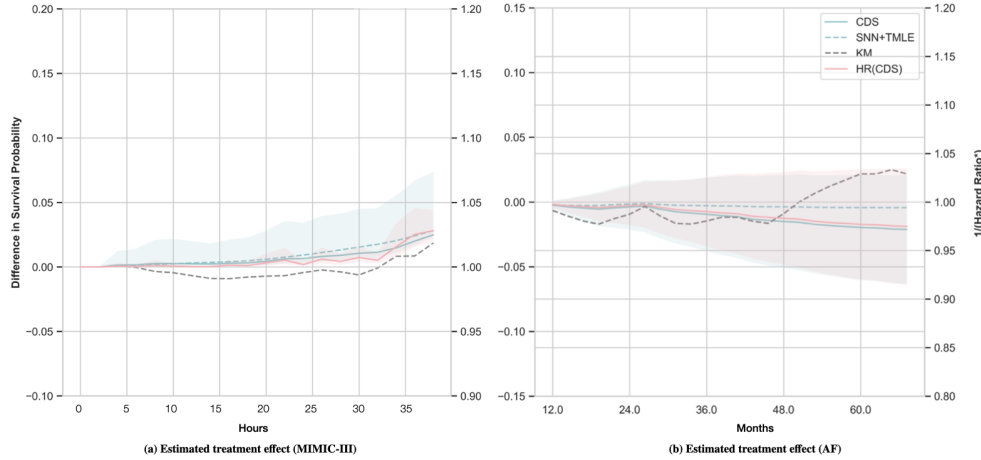


Figure 5: Estimated treatment effect and empirical hazard ratio (HR^*) by benchmark algorithms. The shaded area is the 95% confidence interval of the individual treatment effect estimations. Abbreviations: KM: the Kaplan Meier estimator; TMLE: the SNN model with TMLE adjustment; Hazard Ratio*: the empirical hazard ratio.

However, the heterogeneity of the estimated treatment effect is salient. Figure 6 depicts the distributions of the estimated ITEs using CDS averaged over time and colored by the observed treatment conditions. In the MIMIC-III study, we observed a right skewed distribution of ITEs which favors the use of MV in both treatment groups.

In the AF study, most patients prescribed with VKA (98.95%, 10500/10611) are found with a negative treatment effect and favour the usage of VKA. On the other hand, among patients prescribed with NOAC, we found the time-averaged ITE ranges greatly from -15.45% to 11.27%. There are 60.16% (2730/4538) of the NOAC patients who are estimated with a positive treatment effect and the mean of their time-averaged ITE is 3.14% (3.060%, 3.221%); while for the rest, the mean of the time-averaged ITE is -3.64% (-3.800%, -3.482%). This significant discrepancy between the two groups (i.e., positive and negative treatment effect groups) was concealed when evaluating the ATE but was fully revealed when examining the ITEs.

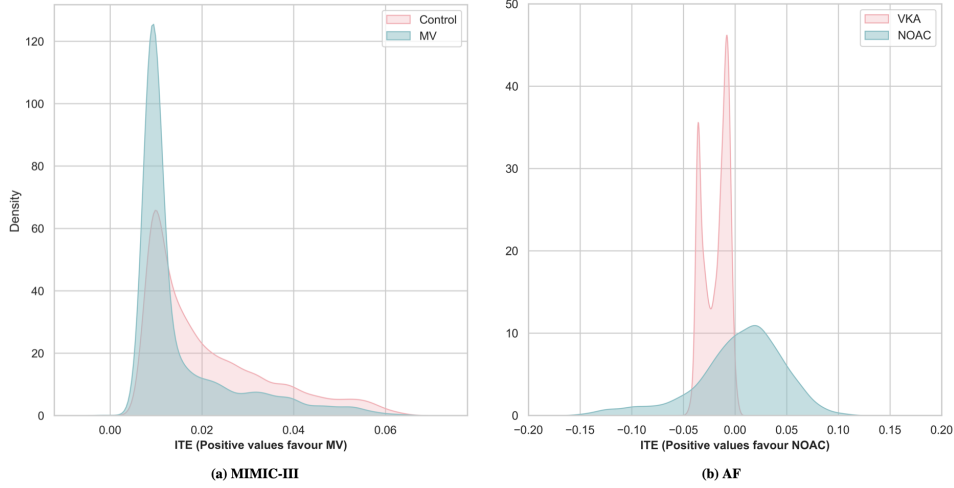


Figure 6: Distributions of estimated individual treatment effects (ITE) averaged over follow-up time. ITE estimations averaged over time in each study. Abbreviations: MV: mechanical ventilation; NOAC: Non-Vitamin K antagonist oral anticoagulants; VKA: Vitamin K antagonists.

4 Discussion

We have developed a novel causal inference algorithm using a causal dynamic survival model, which we call CDS. CDS estimates the individual potential survival response curves from longitudinal observational data. It leverages information across individuals under different interventions with dedicated propensity layers and potential outcome subnetworks. We demonstrated significant gains in the accuracy of CDS over plain recurrent neural networks in estimating individual and conditional average treatment effects.

In addition to extensive simulations, we applied CDS to two observational clinical datasets, the MIMIC-III sepsis study and the CPRD atrial fibrillation study. Compared to the standard neural networks, we found CDS has similar performance for the estimation of survival curves as DeepHit and Super-Learner models (the estimation performance of survival curves is presented in our working paper [32]), but it is superior in identifying the treatment effect heterogeneity over time than existing methods. In particular, CDS estimates the causal effect by computing the adjusted potential survival curves under treatment and control conditions. The use of propensity scores as the input of the network helped to improve the estimation accuracy by correcting for confounding bias. In addition, CDS learns from the pattern of missing confounders of a time series using masking layers rather than imputing their values, and it efficiently captures the epistemic uncertainty from the unknown underlying data generating process by using an ensemble of networks with varied random seeds.

In this study, time-varying confounders have been simulated to resemble the observed data from observational electronic health records. Since deep learning techniques do not assume specific functional dependencies of treatment or outcomes, we expect our simulation results to hold under other choices of functional forms. Nevertheless, more extensive testing of CDS under extreme scenarios such as low overlapping and the presence of unmeasured confounders are desired and left for future work.

Our estimation of confidence intervals for ITEs is conservative and results in a high coverage ratio. However, we observed the interval is responsive to the quality of input data. For scenarios with high levels of overlapping and low levels of sample variance, the corresponding confidence intervals are much narrower. Therefore, the usage of network ensembles effectively captures the model uncertainty.

When comparing the ATE estimation from CDS with that from traditional confounding adjustment methods, we found that using propensity scores as a regressor in the neural network can achieve similar if not better performance than TMLE and IPW. When looking at the estimation performance of ITEs, CDS significantly outperforms both methods.

In our case study, we do not explicitly use confounders captured after the history window. An alternative approach, which would improve the automation and responsiveness of the causal inference analysis, would be to include the full medical history during the estimation period as a time-series input. However, this approach would confuse the interpretation of the treatment effect. That is, how we interpret the treatment effect of a time-varying exposure if the outcome and the exposure are measured in the same time block. This topic is left for future work.

Much of the challenge of longitudinal causal inference lays in its definition of treatment effect. In this study, the treatment effect for a given period t' to Θ has been defined as the difference in survival probability given constant treatment vs. control throughout the history window $t' - u$ to $t' - 1$. However, when we have n treatments, we will face the choice of making the contrast among $n(n - 1)/2$ pairs. Nonetheless, the solution becomes more complicated when we consider the effect of a switch in the treatment, that is, we need to consider the timing of the switch as well as the choice of effect contrast. Similarly, it is also arduous to analyze continuous treatments. Nonparametric methods have been proposed to either discretise treatment options [?] or create splines to estimate the treatment effect on a single day [33]. Few has been discussed for time-varying variables or treatments. One study [27] proposed to use reinforcement learning to control the intravenous fluid dosage for sepsis patients, but it does not answer the question of causal effect nor does it adjust for potential confounding bias. It would be interesting for future studies to explore time-varying deconfounded treatment recommendations.

The proposed model is limited in its ability to capture the bias arising from missing confounders or measurement errors, and cannot be reduced by collecting more data under the same experimental conditions. This is reflected in our scenario analysis where increasing the sample size cannot improve the estimation accuracy if the data lacks overlapping. With observational data, the impact of overlapping is often overlooked due to the limited ability to identify and collect potential confounders. A recent study [34] found 74 out of 87 (85.1%) articles on the impact of alcohol on ischemic heart disease risk spuriously ignored or eventually dismissed confounding in their conclusions. Albeit this study acknowledges the caveats when interpreting results from case studies, it will be important for future researches to quantify the aleatoric uncertainty for data-adaptive models.

CDS fills the gap in causal inference using deep learning techniques for survival analysis. It considers time-varying confounders and binary treatment options. Its treatment effect estimation can be easily compared with conventional literature which uses relative measures of treatment effect. We expect CDS will be particularly useful for identifying and quantifying treatment effect heterogeneity over time under the ever complex observational health care environment.

Acknowledgment

This work was supported by National Health and Medical Research Council, project grant no. 1125414. Ethics to use UK Clinical Practice Research Datalink data was obtained from ISAC (protocol number 17-093).

A Average treatment effect estimation adjustment

A.1 Inverse probability weighting (IPW)

We apply the inverse probability weighting adjustment to the raw estimation of ATE with the following equation:

$$\hat{\psi}_{IPW}(t) = \frac{1}{N} \sum_{i=1}^n \left(\frac{A_i \hat{Y}_i(t)}{\hat{P}(X_i(0))} - \frac{(1 - A_i) \hat{Y}_i(t)}{1 - \hat{P}(X_i(0))} \right), \text{ where } t \in \{0, 1, \dots, \Theta\}$$

where N is the sample size, Θ is the maximum of follow-up time and $\hat{P}(X_i(0))$ is the propensity score estimated as the probability of receiving the treatment at time 0 if the treatment assignment is time-invariant. When the treatment is time-variant, we estimate the propensity score at each time step as $\hat{P}(X_i(t))$. In this study, we estimated $\hat{P}(X_i(0))$ using a densely connected network to fit the binary label of the treatment assignment of each subject i at time 0.

A.2 The iterative targeted maximum likelihood estimation (TMLE)

To apply the iterative targeted maximum likelihood estimation adjustment, we conducted the following adjustment at each time step:

1. We first calculate the smart covariates $H(A, X(t))$ using the propensity score estimated using the procedure aforementioned:

$$H(1, X_i(t)) = \frac{A_i}{\hat{P}(X_i(0))}; H(0, X_i(t)) = \frac{1 - A_i}{1 - \hat{P}(X_i(0))}$$

2. Then we fit the residual of the initial estimate of the logit of the binary label with smart covariates using an intercept-free regression:

$$\text{logit}(\hat{Y}_i(t)) - \text{logit}(Y_i(t)) = \delta_1(t)h(1, X_i(t)) + \delta_0(t)h(0, X_i(t))$$

where $\text{logit}(x)$ represents the function $\log(\frac{x}{1-x})$

3. Calculate the adjusted potential outcomes:

$$\hat{Y}_A(t)^1 = \log\left(\frac{\text{logit}(\hat{Y}_A(t) + \delta_A(t))}{P_A(X_i(0))}\right), \text{ for } A \in \{0, 1\}$$

where $\hat{P}_1(X_i(0)) = \hat{P}(X_i(0))$ and $\hat{P}_0(X_i(0)) = 1 - \hat{P}(X_i(0))$.

4. Targeted estimate of ATE at time t:

$$\hat{\psi}_{TMLE}(t) = \frac{1}{N} \sum_{i=1}^n (\hat{Y}_1(t)^1 - \hat{Y}_0(t)^1)$$

B The structure of the CDS masking and outcome layers

CDS estimates the the difference between potential survival curves under the treatment and control conditions to compute the estimated individual treatment effect (ITE) curve. Here, following the notations in the main manuscript, we describe the masking and outcome layers of the CDS model introduced in Figure 1 as follows:

- A masking layer taking account of informative missingness in longitudinal data [35], which consists of two representations of missing patterns, i.e., a masking vector $M_t \in \{0, 1\}^D$ to denote which variables are missing at time t , and a real vector $\delta_t \in \mathbb{R}^{D, \Theta}$ to capture the time interval for each variable d since its last observation over Θ time points. The masking layer takes as inputs the matrix $[\bar{X}(u), \bar{A}(u)]$ and produces as output a matrix $[\bar{M}(u), \bar{\delta}(u), \bar{X}(u), \bar{A}(u)]$, where the overlines indicate the corresponding vector observed during the history window $[t - u, t - 1]$. This layer effectively uses the missing data patterns to achieve better predictions;
- The potential outcome layers make predictions of the log odds of the binary outcomes given by Y^M given $[\bar{M}(u), \bar{\delta}(u), \bar{X}(u), \bar{A}(u) = 1]$ and $[\bar{M}(u), \bar{\delta}(u), \bar{X}(u), \bar{A}(u) = 0]$ and then convert the log odds into the conditional survival probability to form the potential survival curves under each treatment condition.

C Additional simulation results

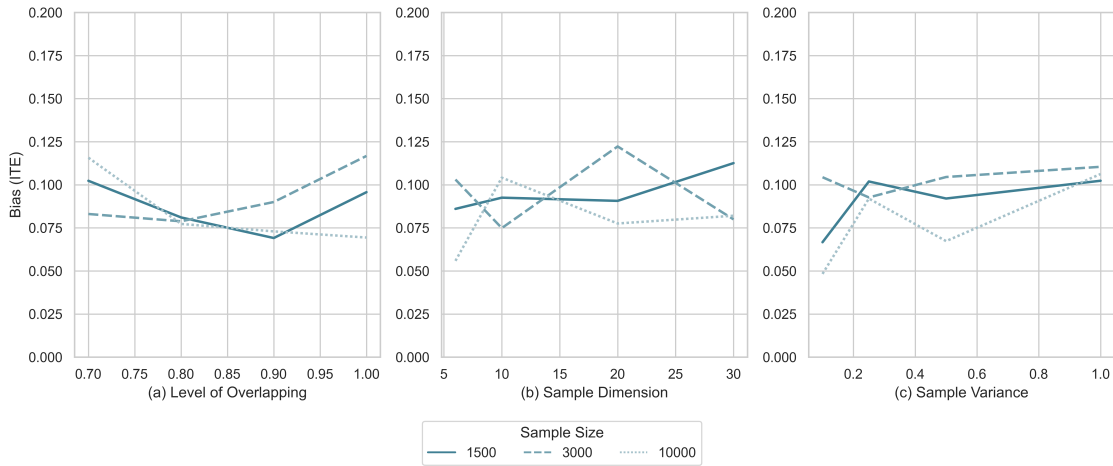


Figure 7: Individual treatment effect (ITE) estimation bias by scenarios. All metrics are averaged across 50 independent simulations over 10 time points from the test dataset under each scenario. Bias: average absolute percentage bias.

References

- [1] Blanca Gallego, Adam G Dunn, and Enrico Coiera. Role of electronic health records in comparative effectiveness research. *Journal of comparative effectiveness research*, 2(6):529–532, 2013.

- [2] T Wendling, K Jung, A Callahan, A Schuler, N H Shah, and B Gallego. Comparing methods for estimation of heterogeneous treatment effects using observational data from health care databases. *Statistics in medicine*, 37(23):3309–3324, 2018.
- [3] Richard L Kravitz, Naihua Duan, and Joel Braslow. Evidence-based medicine, heterogeneity of treatment effects, and the trouble with averages. *The Milbank Quarterly*, 82(4):661–687, 2004.
- [4] Anand Kumar, Daniel Roberts, Kenneth E Wood, Bruce Light, Joseph E Parrillo, Satendra Sharma, Robert Suppes, Daniel Feinstein, Sergio Zanotti, Leo Taiberg, et al. Duration of hypotension before initiation of effective antimicrobial therapy is the critical determinant of survival in human septic shock. *Critical care medicine*, 34(6):1589–1596, 2006.
- [5] Alistair E W Johnson, Jerome Aboab, Jesse D Raffa, Tom J Pollard, Rodrigo O Deliberato, Leo A Celi, and David J Stone. A Comparative Analysis of Sepsis Identification Methods in an Electronic Database*. *Critical Care Medicine*, 46(4):494–499, 2018.
- [6] Michael F Gensheimer and Balasubramanian Narasimhan. A scalable discrete-time survival model for neural networks. *PeerJ*, 7:e6257–e6257, 2019.
- [7] S Rose and M J van der Laan. Targeted Learning: Causal Inference for Observational and Experimental Data. *Targeted Learning: Causal Inference for Observational and Experimental Data*, 2011.
- [8] M Schomaker, M A Luque-Fernandez, V Leroy, and M A Davies. Using longitudinal targeted maximum likelihood estimation in complex settings with dynamic interventions. *Statistics in Medicine*, 2019.
- [9] Changhee Lee, Jinsung Yoon, and Mihaela van der Schaar. Dynamic-DeepHit: A Deep Learning Approach for Dynamic Survival Analysis With Competing Risks Based on Longitudinal Data. *IEEE Transactions on Biomedical Engineering*, 67(1):122–133, 2020.
- [10] Jie Zhu and Blanca Gallego. Targeted Estimation of Heterogeneous Treatment Effect in Observational Survival Analysis. *Journal of Biomedical Informatics*, page 103474, 2020.
- [11] Hans C Van Houwelingen. Dynamic prediction by landmarking in event history analysis. *Scandinavian Journal of Statistics*, 2007.
- [12] C R David. Regression models and life tables (with discussion). *Journal of the Royal Statistical Society*, 34(2):187–220, 1972.
- [13] Julie C Recknor and Alan J Gross. Fitting Survival Data to a Piecewise Linear Hazard Rate in the Presence of Covariates. *Biometrical Journal*, 1994.
- [14] R Henderson. Joint modelling of longitudinal measurements and event time data. *Biostatistics*, 2000.
- [15] Joseph G Ibrahim, Haitao Chu, and Liddy M Chen. Basic concepts and methods for joint models of longitudinal and survival data, 2010.
- [16] Ioana Bica, Ahmed M Alaa, James Jordon, and Mihaela van der Schaar. Estimating counterfactual treatment outcomes over time through adversarially balanced representations. *arXiv preprint arXiv:2002.04083*, 2020.
- [17] John Blitzer, Ryan McDonald, and Fernando Pereira. Domain adaptation with structural correspondence learning. In *COLING/ACL 2006 - EMNLP 2006: 2006 Conference on Empirical Methods in Natural Language Processing, Proceedings of the Conference*, 2006.
- [18] Susan Athey, Julie Tibshirani, and Stefan Wager. Generalized random forests. *The Annals of Statistics*, 47(2):1148–1178, 2019.
- [19] Jie Zhu and Blanca Gallego. Targeted Estimation of Heterogeneous Treatment Effect in Observational Survival Analysis. *Journal of Biomedical Informatics*, page 103474, 2020.
- [20] Kosuke Imai and Aaron Strauss. Estimation of Heterogeneous Treatment Effects from Randomized Experiments, with Application to the Optimal Planning of the Get-Out-the-Vote Campaign. *Political Analysis*, 19(1):1–19, 2011.
- [21] Sepp Hochreiter and Jurgen Schmidhuber. Long short-term memory. *Neural computation*, 9(8):1735–1780, 1997.
- [22] Paul R Rosenbaum and Donald B Rubin. The central role of the propensity score in observational studies for causal effects. *Biometrika*, 70(1):41–55, 1983.
- [23] E Frank, Robert M Harrell, David B Califf, Kerry L Pryor, Robert A Lee, and Rosati. Evaluating the yield of medical tests. *Journal of the American Medical Association*, 247(18):2543–2546, 1982.
- [24] Michael J Crowther and Paul C Lambert. Simulating biologically plausible complex survival data. *Statistics in medicine*, 32(23):4118–4134, 2013.

- [25] A Johnson, T Pollard, and L Shen. MIMIC-III, a freely accessible critical care database. *Sci Data*, 3:160035–160035, 2016.
- [26] C W Seymour. Assessment of clinical criteria for sepsis: For the third international consensus definitions for sepsis and septic shock (sepsis-3). *J Am Med Assoc*, 315:762–774, 2016.
- [27] Matthieu Komorowski, Leo A Celi, Omar Badawi, Anthony C Gordon, and A Aldo Faisal. The Artificial Intelligence Clinician learns optimal treatment strategies for sepsis in intensive care. *Nature Medicine*, 24(11):1716–1720, 2018.
- [28] M Reyna, C Josef, R Jeter, S Shashikumar, B Moody, M B Westover, A Sharma, S Nemati, and G Clifford. Early Prediction of Sepsis from Clinical Data – the PhysioNet Computing in Cardiology Challenge, 2019.
- [29] Emily Herrett, Arlene M Gallagher, Krishnan Bhaskaran, Harriet Forbes, Rohini Mathur, Tjeerd van Staa, and Liam Smeeth. Data Resource Profile: Clinical Practice Research Datalink (CPRD). *International Journal of Epidemiology*, 44(3):827–836, 06 2015.
- [30] Blanca Gallego Luxan and Jie Zhu. Time-to-event comparative effectiveness of noacs vs vkas in newly diagnosed non-valvular atrial fibrillation patients. *medRxiv*, 2021.
- [31] Martin Abadi, Ashish Agarwal, Paul Barham, Eugene Brevdo, Zhifeng Chen, Craig Citro, Greg S Corrado, Andy Davis, Jeffrey Dean, Matthieu Devin, et al. Tensorflow: Large-scale machine learning on heterogeneous distributed systems. *arXiv preprint arXiv:1603.04467*, 2016.
- [32] Jie Zhu and Blanca Gallego. Dynamic prediction of time to event with survival curves, 2021.
- [33] Edward H Kennedy, Zongming Ma, Matthew D McHugh, and Dylan S Small. Nonparametric methods for doubly robust estimation of continuous treatment effects. *Journal of the Royal Statistical Society Series B, Statistical Methodology*, 79(4):1229, 2017.
- [34] Joshua D Wallach, Stylianos Serghiou, Lingzhi Chu, Alexander C Egilman, Vasilis Vasiliou, Joseph S Ross, and John PA Ioannidis. Evaluation of confounding in epidemiologic studies assessing alcohol consumption on the risk of ischemic heart disease. *BMC medical research methodology*, 20(1):1–10, 2020.
- [35] Zhengping Che, Sanjay Purushotham, Kyunghyun Cho, David Sontag, and Yan Liu. Recurrent Neural Networks for Multivariate Time Series with Missing Values. *Scientific Reports*, 8(1):1–12, 2018.